Observations of post-seismic ionospheric disturbances following the great Sumatra event from GPS data

R.Garcia[1], F. Crespon[1,2] and P. Lognonné[1]
(1) Département de Géophysique Spatiale et Planétaire, Institut de Physique du Globe de Paris
(2) Noveltis (Toulouse)
http://ganymede.ipgp.jussieu.fr
garcia@ipgp.jussieu.fr

Introduction:

The coupling of the solid Earth with its atmosphere is responsible of ionospheric perturbations generated after some major earthquakes. These events produce atmospheric infrasounds propagating upward and amplified by the exponential density decrease of the atmosphere. At ionospheric height these acoustic waves generate ionospheric perturbations which can be observed on Total Electronic Content (TEC) along ray paths from GPS receivers to satellites.

A previous study by Ducic et al. (2003) has demonstrated that dense GPS networks are able to detect ionospheric perturbations produced by the seismic surface waves of big Earthquakes, and to derive some constraints on the group velocity of these waves.

We present here the detection of ionospheric perturbations produced by the Great Sumatra earthquake. Such signals are visible above the GPS japanese network (dense network closest to the source), but not seen above European and californian networks. After extracting the ionospheric signal, filtered Slant Total Electron Content (STEC) data exhibit both acoustic and gravity wave signals associated to the quake with a low S/N ratio. We present also a 3D tomography of the ionospheric perturbations generated by the Rayleigh waves.

GPS data and signal extraction:

The TEC signal used in this study has been computed from about 1200 GPS receiver RINEX files from GPS japanese network.

These data have been filtered in two different frequency bands:

- between 3.8 and 7 mHz in order to enhance the infrasonic signal associated to Rayleigh surface waves.
- between 1.0 and 3.3 mHz in the gravity wave frequency band.

As seen on figure 1, the background noise is low in the acoutic frequency band, but increases at lower frequencies in the gravity wave domain.

The ionospheric perturbation produced by Rayleigh seismic surface waves is seen on figure 2 with a poor S/N ratio, but it arrives with in the expected timing and propagate at ~4km/s horizontally (seismic surface wave velocity) and ~1km/s vertically (sound velocity). It's amplitude is of the order of 0.06 TEC unit.

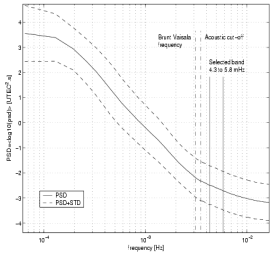

Figure 1: Background noise in STEC GPS data above the Japanese GPS network, averaged over 3 days of data, as a function of frequency

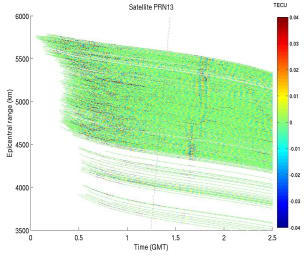

Figure 2: Filtered STEC data along the ray paths from all GPS stations to satellite 13 plotted as a function of time, and epicentral distance between the ionospheric point (along the ray path at 350 km altitude) and the earthquake. The dashed line indicates the arrival time of the surface waves on the groundt, and the bar on the left indicate the vertical scale in TEC units

3D inversion:

The electronic density perturbation model (ΔNe) is estimated from the filtered TEC data (Δ) at each GPS epoch by a least squares inversion (Newton method) of the following linear forward problem: Δ = **G** ΔNe . The matrix **G** is constructed by integration of the electronic density perturbation along a straight line ray from the GPS receiver to the satellite.

The model parameters ΔNe are parametrized by their values in blocks of the model grid computed with a cubed sphere coordinate system. This parametrisation allows an analytical integration along the ray path, and produce blocks that possess approximately the same size. The comparison between this cubed sphere grid and a regular grid in latitude and longitude coordinates is shown on figure 3.

The inverse problem is ill-posed. So, a damping a priori covariance matrix of the model is introduced with diagonal elements 0.1% of the IRI2001 ionospheric model and a 100 km horizontal correlation length. The resolution of the inverse problem is presented on Figure 4. As seen on figures 5 and 6, despite a low S/N ratio, the inverted model is presenting linear features propagating from SW to NE along a great circle at ~4 km/s, an[illegible] at ~1 km/s.

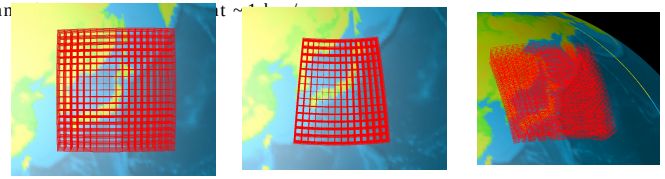

*Figure 3:*Comparison between a cubed sphere grid (right and left panels) and a regular grid in latitude and longitude coodinates (middle panel).

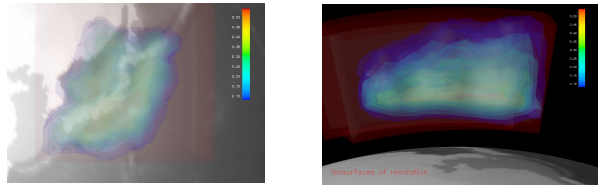

Figure 4: Isosurfaces of the model parameters resolution seen from above (right panel) and from East (left panel). On the left panel the vertical scale is multiplied by a factor 3. The 3 contours indicates the inverted region.

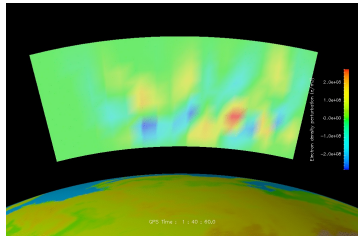

Figure 5: vertical cross section along the great circle path in the inverted model. Vertical sacle is multiplied by a factor 3. Despite the low S/N ratio, inclined wavefronts are visible

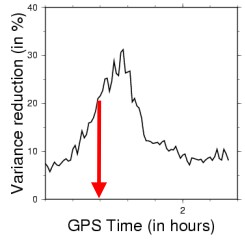

Figure 6: Variance reduction as a function of time. Red arrow indicate the time of the Figure 5 plot

Gravity waves:

The STEC data filtered in the 1.0 to 3.3 mHz are presented in figures 7 and 8 for two different satellites. A strong signal is seen on the left of the figures corresponding probably to a strong Travelling Ionospheric Distrubance.

On the right part of the figures linear features are observed corresponding to waves propagating horizontally at ~200 m/s. The arrival time of these waves (5 hours after the earthquake) is consistent with atmospheric gravity waves produced by the earthquake and the tsunami.

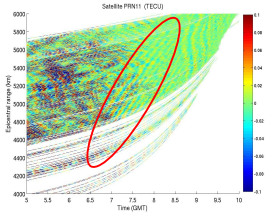

Figure 7: Filtered STEC data along the ray paths from all GPS stations to satellite 11 plotted as a function of time, and epicentral distance between the ionospheric point (along the ray path at 350 km altitude) and the earthquake. The bar on the left indicate the vertical scale in TEC units

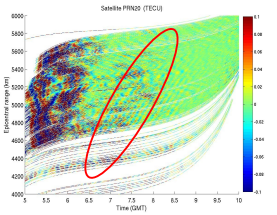

Figure 8: Same as figure 7, Filtered STEC data as a function of time, and ionospheric point epicentral distance for the satellite number 20.

Discussion:

The example of the great Sumatra earthquake is giving an overview of the possible coupling phenomena between the Earth and its atmosphere. The infrasonic waves produced by seismic surface waves are detected and imaged, and the gravity waves are detected. The mechanical coupling between the ground and the upper atmosphere is demonstrated. The 3D ionospheric monitoring of these perturbations is now well defined and appear to be a powerful tool above high density GPS networks.

Unfortunately, this example is also illustrating the drawbacks of ionospheric post-seismic perturbations: the S/N ratio at far field is large enough only for earthquake magnitude greater than 8.0, the atmospheric gravity waves generated by the tsunami are hidden in the background TID noise, and the resolution of the inverse problem is low.

However, the data base of ionospheric post-seismic signals is increasing and will allow the extraction of seismic surface wave velocities in order to perform lithospheric tomography studies.

Conclusion:

A 3D mapping of the postseismic ionospheric perturbations observed on TEC GPS data has been obtained. These electronic density perturbations are related to infrasounds produced by a Rayleigh seismic surface wave and to atmospheric gravity waves produced by the tsunami.

The spatial resolution of the 3D picture is limited by the spatial extent of the GPS network, the density of GPS receivers and the limited number of satellites. These resolution problems will soon be solved by the extent of GPS networks and the advent of Galileo system. The next challenges are the modeling of interactions between infrasonic (or gravity) waves and the ionosphere in order to recover the source signal from electronic density perturbations, and the definition of a new observing system dedicated to such phenomena above the ocean where other seismic observations are missing.

Acknowledgements: We thank Makoto Murakami from GSI for his collaboration on the GPS data from Japanese network.

References:
- Garcia R., F. Crespon, V. Ducic, P. Lognonne, in revision, 3D tomography of post-seismic perturbations produced by the Denali earthquake from GPS data, Geophys. J. Int.
- Ducic V., J. Artru and P. Lognonné, 2003, Ionospheric remote sensing of the Denali Earthquake Rayleigh surface waves, Geophys. Res. Lett., v. 30, n. 18, doi: 10.1029/2003GL017812